

# **B. TECH PROJECT REPORT**

**On**

**IMAGE PROCESSING ON  
MEDICAL IMAGES OF CT  
SCAN OF LUNGS**

**BY**

**VARAKALA.VATHSALYA SPOORTHY**

**190002064**



**DISCIPLINE OF CIVIL ENGINEERING**

**INDIAN INSTITUTE OF TECHNOLOGY INDORE**

**November 2022**

**IMAGE PROCESSING ON MEDICAL  
IMAGES OF CT SCAN OF LUNGS  
PROJECT REPORT**

*Submitted in partial fulfillment of the requirements for  
the award of the degrees*

of

**BACHELOR OF TECHNOLOGY**

**In**

**ELECTRICAL ENGINEERING**

*Submitted by:*

**Varakala.Vathsalya Spoorthi**

*Guided by:*

**Dr. SRIVATSAN VASUDEVAN**

Associate Professor,

Department of Electrical Engineering,

IIT Indore



**INDIAN INSTITUTE OF TECHNOLOGY INDORE**

**November 2022**

## **CANDIDATE'S DECLARATION**

I hereby declare that the project entitled IMAGE PROCESSING ON MEDICAL IMAGES OF CT SCAN OF LUNGS submitted in partial fulfillment for the award of the degree of Bachelor of Technology in "Electrical Engineering" completed under the supervision of Dr. Srivathsan Vasudevan, Associate Professor, Department of Electrical Engineering, IIT Indore is an original work.

Further, I declare that I have not submitted this work for the award of any other Degree elsewhere.

V.Vathsalya  
Spoorthi  
29/11/22

**Varakala.Vathsalya Spoorthi**


**29/11/22**

**Signature and name of the student(s) with the date**

---

## **CERTIFICATE by BTP Guide(s)**

It is certified that the above statement made by the students is correct to the best of my knowledge.

  
Dr. Srivathsan Vasudevan,  
Associate Professor,  
Discipline of Electrical Engineering,  
IIT Indore

**Signature of BTP Guide(s) with dates and their designation**

## **Preface**

This report on Image Processing on medical images of CT Scan of lungs

has been prepared as a part of my B.Tech Project under the guidance of Dr. Srivathsan Vasudevan, Associate Professor, Department of Electrical Engineering, Indian Institute of Technology, Indore.

Through this project, I have given a detailed explanation of Stewart platform and their mechanical, electrical design. Which we are going to use as microcontroller which can mimic the movement of the tumor in lungs and further will be helpful in treatment of lung cancer.

I have tried to the best of my abilities and knowledge to explain the content lucidly. I have also used tables, figures, and flow charts to make it more illustrative.

**Varakala.Vathsalya Spoorthi**

**190002064**

**B.Tech 4<sup>th</sup> Year**

**The discipline of Electrical Engineering**

**IIT Indore**

### **Acknowledgments**

I would like to thank Dr. Srivathsan Vasudevan for his support, valuable guidance. I sincerely thank him for his efforts and patience.

I also wish to thank Ph.D. Scholar Suhel Khan for his full support and guidance throughout the project. He provided me with all the resources required for the study and was also available for me whenever I needed his guidance.

Without their support, this report would not have been possible.

**Varakala.Vathsalya Spoorthi**

**190002064**

**B.Tech 4<sup>th</sup> Year**

**The discipline of Civil Engineering**

**IIT Indore**

## **ABSTRACT**

Lung cancer is one of the world's most deadly and life-threatening diseases. It is also one of the most common cancers in the world with a very low survival rate of 18.6%. Early detection plays a very important role in effective treatment of this disease. Detection of lung cancer is done by interpreting images obtained by an imaging technique called Computed Tomography(CT). CT Scan has been one of the greatest medical imaging tools used in the medical sector. But the visual interpretation and detection of cancer from CT scan images is difficult even for physicians. Image processing techniques have sparked interest in the interpretation of CT scan images of lung cancer cells in recent years. MATLAB was utilized in this research for most of the image processing techniques. The aim of this project is to use image processing techniques for tracking of tumor location during expansion and contraction of lungs and implement a microcontroller based system to mimic the way the tumor moves inside the lungs and use this data to help in precise radiation treatment. As a part of the treatment, Radiation is applied on lung cells to kill the cancerous cells but as long as the precise location of tumor inside the lungs is not known, Radiation may damage healthy cells. Hence tracking of tumor location using image processing techniques helps reduce radiation intensity applied on lungs during treatment and saves healthy cells from radiation. Through this project, I have given a detailed explanation of Stewart platform and their mechanical, electrical design. Which we are going to use as microcontroller which can mimic the movement of the tumor in lungs and further will be helpful in treatment of lung cancer.



## [\Contents](#)

CANDIDATES' DECLARATION	iii
CERTIFICATE BY BTP GUDE	iii
PREFACE	iv
ACKNOWLEDGEMENTS	v
ABSTRACT.....	vi
<b>1 Introduction.....</b>	<b>1</b>
<b>1.1 Background.....</b>	<b>2</b>
<b>1.3 Objective .....</b>	<b>2</b>
<b>2 Literature Review .....</b>	<b>3</b>
<b>3 Stewart Platform .....</b>	<b>4</b>
<b>3.a Overview Of Robots.....</b>	<b>4</b>
<b>3.b Parallel Robots .....</b>	<b>5</b>
<b>3.c Stewart Platform.....</b>	<b>6</b>
<b>3.c.1 Hisrory.....</b>	<b>8</b>
<b>3.c.2 Kinematic Equations .....</b>	<b>9</b>
<b>4 Mechanical Design.....</b>	<b>15</b>
<b>4.1 Linear Actuators .....</b>	<b>15</b>
<b>4.2Magnetic Spherical Joints .....</b>	<b>18</b>
<b>4.3 Platform.....</b>	<b>20</b>
<b>4.4 Shaft Couplers .....</b>	<b>20</b>
<b>4.5 6 – 3Configuration Geometry .....</b>	<b>21</b>
<b>4.6 Electronic Enclosure.....</b>	<b>23</b>
<b>5. Electronic Design.....</b>	<b>25</b>
<b>5.a Microcontroller.....</b>	<b>26</b>
<b>5.a.1 MicroController Selection.....</b>	<b>26</b>
<b>5.a.2 Arduino Due Specification.....</b>	<b>27</b>
<b>5.b Hexamoto Sheild.....</b>	<b>28</b>

5.b.1 Design Requirements.....	28
5.b.2Hexa Moto Design.....	30
5.b.3 Component Detail.....	30
5.b.3.aSTMicroelectronic I9958SBTRMotor Drive.....	30
5.b.3.bl/O Hardware Component's.....	32
5.c HexaMoto Shield Asembly.....	33
5.d DC Power Supply.....	34
5.e Connectors.....	35
6 Conclusion and Future work.....	<b>Error! Bookmark not defined.</b>
7 References.....	<b>Error! Bookmark not defined.</b>



## **List of Figures**

Figure 1 Closed and Open kinematic loop Mechanics.....	5
Figure 2 Stewart platform Configuration.....	7
Figure 3. Typical Stewart Platform Configuration.....	7
Figure 4 Unstable 6-6 configuration.....	8
Figure 5 Tyre testing Application of Stewart Platform.....	9
Figure 6 Home position of Stewart Platform Robot.....	9
Figure 7 Section view of an Electric actuator.....	16
Figure 8 Ball Joint Rod Ends.....	18
Figure 9. Magnetic Spherical Joint Configuration.....	19
Figure 10 Hellical WAC 20mm-4mm- 4mm Couplings.....	21
Figure 11 Range Of Motion Limitation with Sharing Spherical Joint.....	22
Figure 12 Joint angle of spherical joint in 6-3 configuration.....	23
Figure 13 Examples of Electronic Enclosure and Arduino Due Mount.....	24
Figure 14 Molex Connector Retainer and Label.....	24
Figure 15 Stewart Platform System Design.....	25
Figure 16 Arduino Due.....	27
Figure 17 Progressive Automation PA -14p Pinout [19].....	29
Figure 18 L9958 Block Diagram and PowerSO16 Pinout [22].....	31
Figure 19 L9958 Application Circuit [22].....	31
Figure 20 HexaMoto Shield I/O Hardware.....	32
Figure 21 Hexamoto Shield ,post solder paste application and reflow.....	33
Figure 22 HexaMoto Shield Completed.....	34
Figure 23 PA -14P Current Drawn Vs load[19].....	35
Figure 24 Power and USB Receptile connector Enclosure.....	36
Figure 25 MicroUSB to USB-B connector.....	36

## **LIST OF TABLES**

1. <b>Table 1</b> Arduino Due Technical specifications.....	27
---	----

.

## **Chapter 1**

### **Introduction**

#### **1.1 Background**

One of the most hazardous diseases in the world is lung cancer. Non-small cell and small cell lung cancer are the 2 primary subtypes that are typically recognised. They develop differently and are handled differently depending on the type of lung cancer(LC). Compared to small cell lung cancer, non-small cell lung cancer is more prevalent. Depending on how it manifests and spreads, LC is treated in several ways. Chemotherapy ,Surgery, radiation therapy or a combination of these treatments that may be used to treat non-small cell lung cancer patients. Chemotherapy ,Radiation treatment are typically used to cure patients with small cell lung cancer.

One of the most hazardous diseases in the world is lung cancer. Typically, there are two basic forms of lung cancer: small cell and. Various imaging techniques are available today for detection of lung cancer like CT (Computed Tomography),PET (Positron emission Tomography),magnetic resonance etc.,. Out of the available techniques, low dose CT is considered the gold standard for diagnosis of LC. Image processing techniques are broadly used in the detection phase to assist for early medical therapy in a range of medical conditions. As a result, it's worth contemplating the usage of a Computer-Aided Identification system that uses CT images to aid in the early detection of LC. There are different methods to treat LC such as radiation therapy, chemotherapy, surgery etc., . Radiation therapy is an area constrained treatment. Hence, unlike other cancer treatments which can cause damage to cells all over the body, Radiation therapy allows medical professionals to work on specific parts of the body. Out of all the procedures to treat lung cancer, Radiation therapy has been proved to be the most effective one

During Radiation Therapy(RT), high doses of radiation are used to destroy cancer cells and also contract tumors. Inside cancer cells, radiation damages genetic material called DNA .This occurs by creating small breaks in genetic material. If a cancer cell can't repair its DNA, it won't be able to reproduce new cells, hence they no longer have the ability to divide and grow and will eventually die. Body will naturally get rid of these cancer

cells. Radiation is highly effective in killing actively dividing cells. Cancer cells divide more quickly as compared to normal body cells and they do not have the ability to repair themselves as quickly as normal human body cells. These characteristics of cancer cells make them more susceptible to radiation. Radiation therapy may be recommended by a doctor for a variety of reasons such as decreasing or curing cancer in its early stages, preventing cancer from spreading out to other parts of the body, treating cancer that has returned, alleviating advanced cancer symptoms. Different treatment goals can be met with radiation therapy. It can improve the effectiveness of surgery, prevent cancer from spreading, or treat symptoms of advanced cancer.

## **1.2 Motivation of work**

Radiation therapy has been the most successful treatment for lung cancer but it not only kills or delays cancer cells, it can also harm healthy or non cancerous cells nearby. Damage to healthy cells can have negative consequences. Radiation therapies are designed to kill cancer cells while causing the least amount of harm to neighboring healthy cells. Hence, making radiation therapy more precise is the objective of this project. Radiation therapy preparation focuses on accurately focusing the radiation dose to the tumor to minimize adverse effects and avoid damaging normal cells. For making radiation therapy more precise, it is important to track down the exact location of the tumor. Imaging tests and image processing techniques combined can work effectively to track location of tumor and also determine its shape. So objective of this project is to collect CT scan images of patient suffering from lung cancer. Track the location of lung tumor using image processing techniques. Use the image processing data of tumor location and mimic the movement of tumor using a microcontroller based system for precise radiation therapy

## **1.3 Objective**

Radiation Therapy is usually used for the treatments of lung cancer in stage 1 mainly and sometimes based on the patient requirements it can also be used in stage 2 (quite less). Our main focus here is on the stage 1 of the lung cancer where the tumor is of size 3cm or less (i.e., diameter of tumor is 3cm or less) or 4cm. Therefore in this project we are going to prepare a microcontroller based system which can mimic the tumor in lungs based on the image processing data and to use Steward platform as microcontroller based system which can mimic the tumor.

## Chapter 2

### Literature Review

In traditional radiation therapy, doctors or other healthcare providers determine the tumour location using visual interpretation of CT scan images before starting radiation treatment. Consequently, radiation is administered in traditional radiation therapy due to lack of precision, to tumour cells and surrounding regions. Damage to nearby, healthy, non-cancerous cells results from this. The patient may experience serious adverse effects from this, which occasionally have a fatal outcome. Therefore, a research of enhanced radiation therapy precision is of relevance. Image guided radiation therapy is one step toward high precision radiation therapy. The technique known as "image guided radiation therapy" refers to the use of various imaging technologies in the design and delivery of radiation therapy, and it is becoming more and more crucial in the treatment of cancer patients getting radiation therapy. With high-intensity radiation dose deposition targeted to the precise target structures and minimal radiation dose deposited in nearby normal tissues, image-guided radiation treatment is a recent development in the ongoing effort to improve targeting capabilities. The targeting discrimination could be substantially enhanced to increase the therapeutic ratio. Radiation therapy with image guidance is used to treat malignancies in the lungs and other actively moving body components. Imaging technology used by radiation therapy equipment enables medical personnel to view the tumour both during and after treatment. By comparing these images to that of the reference images captured while simulation, the patient's positions and/or the radiation beams may be altered to precisely target the radiation dose to the tumour. In order to reduce the amount of healthy tissue treated and increase the dose to the tumour, image guided radiation therapy allows for the measurement of changes in tumour position, size, and form throughout treatment. Adjustments are made to maximise geometric accuracy and precision of radiation administration. These geometric benefits enhance tumour management, reduce the possibility of radiation therapy-related toxicity, and facilitate the design of more compact treatment plans.

## Chapter 3

### Stewart platform

#### 3.a Overview of Robots

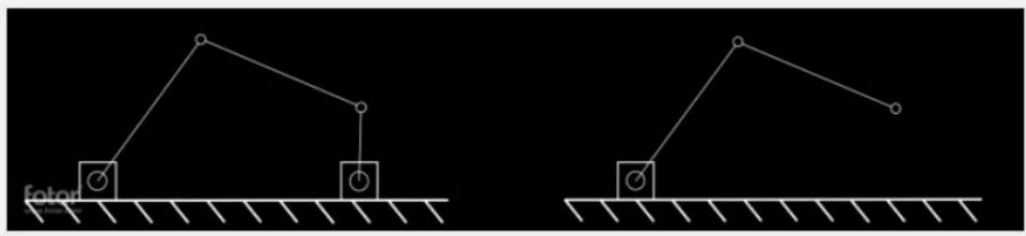
A machine which can be easily instructed to carry out a series of activities automatically, usually by a computer is a robot. Robots come in a huge range of sizes, abilities, prices, and ways of working. They typically consist of a number of actuators and links that link to an end effector to form kinematic chains. A tool attached to the end of a robotic system is called an end effector. There are six degrees of freedom, or ways in which the end effector can move in space (DOF). Translation has three degrees of freedom and takes place along X, Y, and Z, which are mutually orthogonal axes. Rotation about these three axes may add an additional three degrees of freedom. To precisely specify the location and orientation of the object, these six DOF are required.

The connection between links that permits mobility is known as a joint. This movement may be circular, rotational, or linear. Linear motors, cylinders powered by fluid, and electric linear actuators (ELA) are a few examples of linear joints. Through the use of gearing, an ELA is hinged by a screw mechanism. Similar in operation to a rotary motor, a linear motor's stator and rotor are "unfolded" to enable linear but limited movement. It's crucial to remember that a joint does not require total control. Practice makes it challenging to regulate spherical joints. Additionally, pneumatic joints are ideal for actuating to the retracted and extended positions of the cylinder, but it is more challenging to precisely control their actuation to intermediate locations. Links are stiff components that join a robot's joints.

In robotic research and analysis, forward and inverse kinematics play a key role. Given all joint values, forward kinematics enables the end effector's position and orientation to be known. Given an end effector orientation and position that is known or desired, inverse kinematics calculates the joint values. In robotic research and analysis, forward and inverse kinematics play a key role. Given all joint values, forward kinematics enables the end effector's orientation and position to be known. Given an end effector orientation and



position that is known or desired, inverse kinematics calculates the joint values. A kinematic loop is made up of joints and links and can be either closed or open. When links are joined in serial fashion via joints, an open kinematic loop results. Each link, including ground, must be connected to at least two additional links in order for the kinematic loop to be considered closed. A typical mechanism with a closed kinematic loop is a four-bar linkage. An example of an open loop mechanism is the arm of an excavator.



1) CKL(Closed Kinematic loop )

2) OKL(Open Kinematic loop)

**Fig .1 CKL and OKL Mechanisms**

### **3.b Parallel Robots(PR)**

A parallel general manipulator is a "closed-loop kinematic chain mechanism whose end effector is coupled to the base by numerous distinct kinematic chains". The manipulator becomes an n-degrees-of-freedom robot when controlled actuation occurs through n actuators. A parallel robot's unique properties, analysis, and behaviour are all a result of this geometry. Parallel robots have different structures and up to six degrees of freedom.

It is crucial to contrast the distinctions b/w parallel and serial robots and highlight the capabilities of each kind of robot. The payload-to-mass ratio of a robot, which is often larger for PR, is a significant attribute. This is because a parallel robot was built in a closed-loop system. This architecture can withstand higher forces associated with increased mass or acceleration since the robot loading is distributed across its actuators. In contrast, a serial robot's open-loop design gradually raises the force applied to each joint. Only the end effector's mass and inertial forces should be supported by the wrist, which is the body's outermost joint. The wrist joint, the end effector, and the forearm link must all be supported by the next joint, the elbow. This keeps going all the way to the robot's base. An open loop mechanism under load may deform without being seen by sensors, it lowers positional

accuracy. The serial robot must be extremely stiff to make up for this, and the overdesigned geometry adds to the robot's weight. When compared to serial robots of the same size, parallel robots typically have lower workspace because to their higher stiffness and payload-to-mass ratios.

For a serial robot, the forward kinematics equations can be simply solved, but the inverse kinematics solutions are substantially more complex. In contrast, a parallel robot's inverse kinematics solution requires substantially less work than its forward kinematics solution, a topic of continuing research for particular varieties of parallel robotics.

### **3.c Stewart platform**

A typical parallel manipulator with 6 dof is the Stewart Platform. The general Stewart-Gough platform, according to Cruz, Ferreira, and Sequeira [5], is made up of 2 rigid bodies coupled by an amount of prismatic actuators in a parallel arrangement of kinematic chains. Typically, 6 actuators are employed to connect random spots in the two bodies.

Spherical or universal joints are used to connect the actuators to the stiff bodies. In this case, the Stewart Platform would be an SPS, or spherical-prismatic-spherical, robot. Although the joint placements are flexible, uniformly spaced joints produce unique situations. A 6-6 design is when the joints are  $60^\circ$  apart all the way around the movable platform and the base. A 6-3 configuration is when two actuators are joined to the same joint and are kept apart by  $120^\circ$  on the moving platform. A 3-3 layout is achieved by spreading the top and bottom platforms by 120 degrees, as shown below.

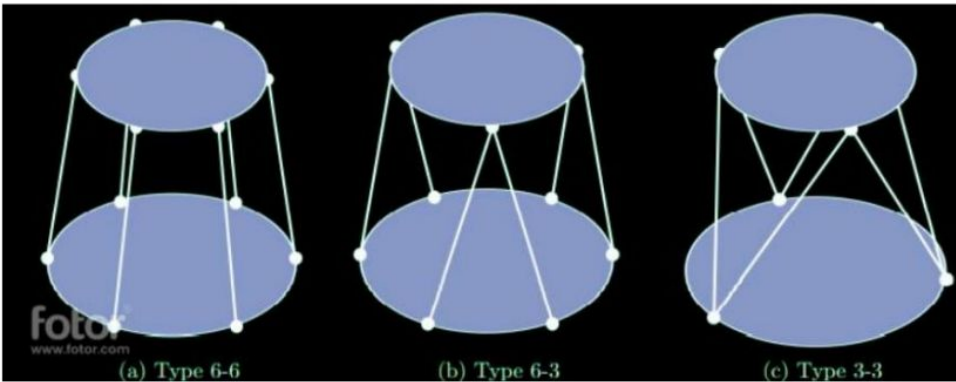


**Fig .2 Stewart Platform configurations**

A right type 6-6 Stewart Platform was never discovered to be deployed in practise in a literature review. Platforms were typically created using a combination of the 6-6 and 3-3 configurations. Each actuator had its own joint, similar to how they would in a 6-6 arrangement, and pairs of joints were kept apart by a little space, giving the geometry a look like Type 3-3. Below is a diagram of this geometry.

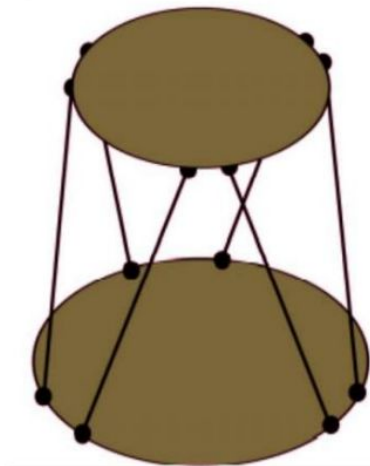


**Fig.3 TSP( Typical Stewart platform) Joint configuration**

A genuine 6-6 platform with  $60^\circ$  between each joint is unstable, according to further analysis. It allows the top platform to revolve about its axis due to the lack of force balance. The image below illustrates this. The links can't exert forces in opposing directions in the presence of a little disturbance, which causes a pair to form around the links. Spherical joints

collapse because they are unable to withstand this situation. This flaw in a true 6-6 layout highlights the benefits of 6-3, 3-3, and similar geometries.

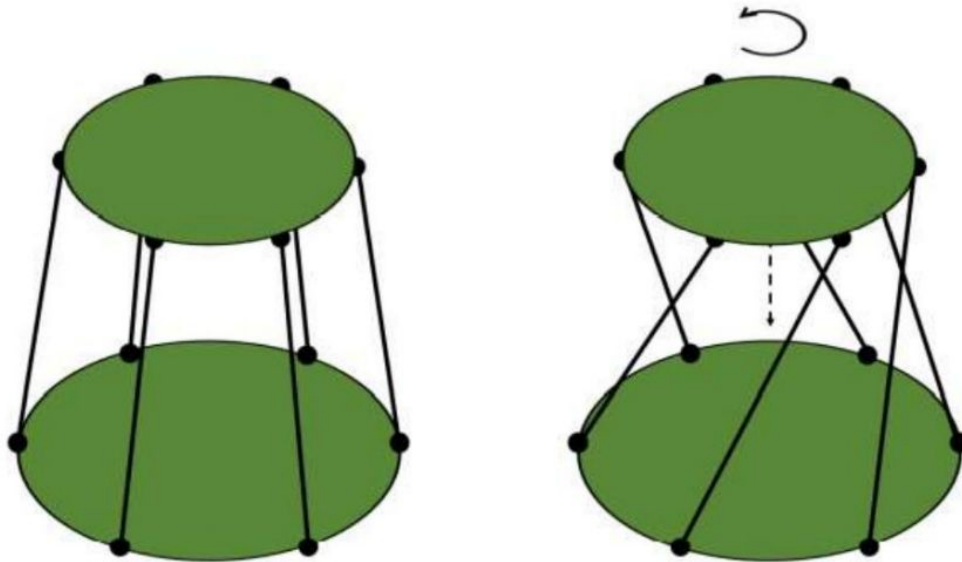


**Fig.4 Unstable 6-6 Configuration**

### 3.c.1 History

Serial robots draw inspiration from the human arm and its utility further dominating the early stages of robotics. Parallel robots are now the subject of additional research and development, notably in industry in recent years, thanks to Stewart and Gough's efforts. Eric Gough developed a CLK system and its guiding principles in 1947, and in 1955, he constructed a prototype for tyre testing, according to Merlet [15]. The development of aviation in the 1960s led to a requirement for flight simulators. In 1965, Stewart wrote "A Platform with Six Degrees of Freedom," in which he discussed designing the simulators' triangle parallel mechanisms. Stewart made significant contributions to the creation of flight simulators, although his published concept was never used. However, Stewart's work was evaluated and Gough created a tire-testing apparatus that was widely utilised in industry. The Gough Tire Testing Machine, which used six jacks to provide combined loads to test Dunlop tyres, is seen in the figure below. Whatever the case, the platform is now known as the Stewart-Gough Platform or, more commonly, the Stewart Platform



**Fig.5 Tyre Testing Application of Stewart Platform**

### **3.c.2 Kinematic Equations**

The six kinematic chains of the SP(Stewart Platform) are analysed to yield the platform's kinematics. The inverse kinematic derivation of the Stewart Platform by Dr. Saeed Niku is used in the following derivation, which can be found in the third edition of his book Introduction to Robotics: Analysis, Control, Applications [17].

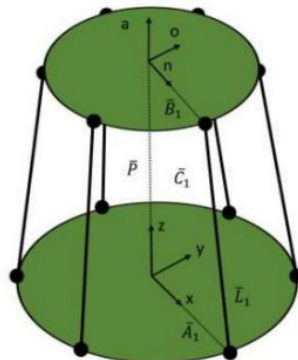


**Fig.6 6-6 configuration of Stewart platform Robot**



The base of the platform is equipped with a stable reference frame xyz in the middle. The x-axis is parallel to the base and oriented toward a spherical joint whereas the z-axis is perpendicular to the base.

Similar to this, movable reference frame noa is positioned in the middle of the moving platform with the n-axis pointing in the direction of a spherical joint and the a-axis normal to the face of the moving platform. It is expected that the linear actuator serves as the connection between the spherical joints. Rotation of frame noa is by  $\alpha$ ,  $\beta$ , and  $\gamma$ , respectively.

Each kinematic chain is made up of four components. C: At an angle from x, A connects the fixed reference frame's origin and the base spherical joint. At an angle from n, B connects the moving platform's spherical joint origin to the moving reference frame's origin. The spherical joints are joined by L. P, which is shared by all six chains, links the two frames' origins. Given the location P and orientation of frame noa, the goal of IK( inverse kinematics) is to calculate the length L of each linear actuator.

Each actuator's length is determined by the vector equation, which is

$$\overline{L_i} = \overline{P} + \overline{B_i} - \overline{A_i} \quad (1.1)$$

For chain C1, A1 and B1 lie along the x and n axes, respectively, and their angles are zero. for  $i = 1..6$ . Subsequent chains on a Type 6-6 SP will be 60 degrees x away from the x and n axes. In practise, Stewart Platforms will have some degree of symmetry; however, this is not always the case and the remaining angles can have any value.  $\alpha_i$  for the general case can be stated as by adhering to the vector convention in Introduction to Robotics by Dr. Saeed Niku [16].

$\alpha_i$  for the general case can be written as

$$\overline{A_i} = \begin{bmatrix} A \cos(\alpha_i) \\ A \sin(\alpha_i) \\ 0 \\ 1 \end{bmatrix} \quad (1.2)$$

where  $A_i$ 's angle with the x axis is represented by the  $i$ th term.

$A_i$  for  $i=1..6$  will be constant during the Stewart Platform's motion.

a specific geometry

Likewise,  $B_i$  can be expressed as

$$\overline{B_i} = \begin{bmatrix} B \cos(i_{th}) \\ B \sin(i_{th}) \\ 0 \\ 1 \end{bmatrix} \quad (1.3)$$

in the moving platform's home location, as depicted in Figure 1.6. After the robot has been calibrated and all of the actuators have been shortened to their shortest length, the home position is reached.

$B_i$ 's components will alter when the platform rotates because it is connected to the rotating frame noa. Rotation matrices must be pre-multiplied to  $B_i$ . in order to take this rotation into account.



The rotation matrices are constructed by using the variables from the moving reference frame.

$$Rot(x, \theta) = \begin{bmatrix} 1 & 0 & 0 \\ 0 & \cos\theta & -\sin\theta \\ 0 & \sin\theta & \cos\theta \end{bmatrix} \quad (1.4)$$

$$Rot(y, \phi) = \begin{bmatrix} \cos\phi & 0 & \sin\phi \\ 0 & 1 & 0 \\ -\sin\phi & 0 & \cos\phi \end{bmatrix} \quad (1.5)$$

$$Rot(z, \psi) = \begin{bmatrix} \cos\psi & -\sin\psi & 0 \\ \sin\psi & \cos\psi & 0 \\ 0 & 0 & 1 \end{bmatrix} \quad (1.6)$$

Equations 1.4, 1.5, and 1.6 are taken from Introduction to Robotics [16]'s equations 2.20 and 2.21. Only rotation is taken into account by these 3x3 rotation matrices. They can be stretched to 4x4 to accommodate positions where the fourth row and column are both zero, with the exception of element 4,4, which has a value of one.

Each kinematic chain's value of  $B_i$  after rotation should be pre-multiplied to the aforementioned rotation matrices to obtain the following result:

$$\begin{bmatrix} B_ix \\ B_iy \\ B_iz \\ 1 \end{bmatrix}_{rot} = \begin{bmatrix} Rot(z, \psi) \end{bmatrix} \begin{bmatrix} Rot(y, \psi) \end{bmatrix} \begin{bmatrix} Rot(x, \theta) \end{bmatrix} \begin{bmatrix} B_ix \\ B_iy \\ B_iz \\ 1 \end{bmatrix}_{home} \quad (1.7)$$

Multiplying  $Rot(z, \psi)$  and  $Rot(y, \phi)$  yields

$$\begin{bmatrix} Rot(z, \psi) \end{bmatrix} \begin{bmatrix} Rot(y, \psi) \end{bmatrix} = \begin{bmatrix} \cos\phi\cos\psi & -\sin\psi & \cos\psi\sin\phi \\ \cos\phi\sin\psi & \cos\psi & \sin\phi\sin\psi \\ -\sin\phi & 0 & \cos\phi \end{bmatrix} \quad (1.8)$$

$$\begin{bmatrix} \cos\phi\cos\psi & -\sin\psi & \cos\psi\sin\phi \\ \cos\phi\sin\psi & \cos\psi & \sin\phi\sin\psi \\ -\sin\phi & 0 & \cos\phi \end{bmatrix} \begin{bmatrix} 1 & 0 & 0 \\ 0 & \cos\theta & -\sin\theta \\ 0 & \sin\theta & \cos\theta \end{bmatrix} =$$

$$\begin{bmatrix} \cos\phi\cos\psi & \cos\psi\sin\phi\sin\theta - \cos\theta\sin\psi & \sin\psi\sin\theta + \cos\psi\cos\theta\sin\phi \\ \cos\phi\sin\psi & \cos\psi\cos\theta + \sin\phi\sin\psi\sin\theta & \cos\theta\sin\phi\sin\psi - \cos\psi\sin\theta \\ -\sin\phi & \cos\phi\sin\theta & \cos\phi\cos\theta \end{bmatrix} \quad (1.9)$$

After combining the rotation matrices, Equation 1.7 becomes

$$\begin{bmatrix} B_ix \\ B_iy \\ B_iz \\ 1 \end{bmatrix}_{rot} = \begin{bmatrix} \cos\phi\cos\psi & \cos\psi\sin\phi\sin\theta - \cos\theta\sin\psi & \sin\psi\sin\theta + \cos\psi\cos\theta\sin\phi & 0 \\ \cos\phi\sin\psi & \cos\psi\cos\theta + \sin\phi\sin\psi\sin\theta & \cos\theta\sin\phi\sin\psi - \cos\psi\sin\theta & 0 \\ -\sin\phi & \cos\phi\sin\theta & \cos\phi\cos\theta & 0 \\ 0 & 0 & 0 & 1 \end{bmatrix} \begin{bmatrix} B_ix \\ B_iy \\ B_iz \\ 1 \end{bmatrix}_{home} \quad (1.10)$$

$\theta, \varphi, \psi$ , are known when moving platform orientation is specified, and  $[B_i]_{\text{home}}$  is known from the St geometry. As a result,  $[B_i]_{\text{rot}}$  can be fixed. Equation 1.1's vectors can be expanded into component form to produce

$$\begin{bmatrix} L_{ix} \\ L_{iy} \\ L_{iz} \end{bmatrix} = \begin{bmatrix} P_{ix} \\ P_{iy} \\ P_{iz} \end{bmatrix} + \begin{bmatrix} B_{ix} \\ B_{iy} \\ B_{iz} \end{bmatrix} - \begin{bmatrix} A_{ix} \\ A_{iy} \\ A_{iz} \end{bmatrix} \quad (1.11)$$

for  $i=1..6$ .

The required quantity derived from the kinematics is the lengths of the linear actuators. Each length's magnitude is determined by

$$|L_i| = \sqrt{(L_{ix})^2 + (L_{iy})^2 + (L_{iz})^2} \quad (1.12)$$

for  $i=1..6$ .

The setpoints for controlling the Stewart Platform are determined by these estimated lengths.

## Chapter 4

### **Mechanical Design**

The mechanical layout of the SP had a number of significant focal points. The first was to design a platform that could be quickly put together and taken apart to produce different combinations. The three main configurations of the Stewart Platform are 6-6, 6-3, and 3-3. The Stewart Platform was created to be easily reconfigurable in a matter of minutes using just a hex key in order to avoid being restricted to a single configuration.

#### **4.1 Linear Actuators**

A linear actuator's fundamental function is to move anything along an axis. Typically, hydraulic, pneumatic, or electrical power can do this. The SP, in particular its intended lab setting and performance requirements, were taken into consideration when evaluating these actuation mediums. Because the controlled variables used to actuate the SP are joint lengths, the linear actuators that drive it must have some sort of positional feedback. The Stewart Platform's actuators, which must be able to sustain and move cargo, are predominantly vertically orientated.

The words stroke, force, and speed are frequently used while discussing linear actuators. The stroke is the separation b/w the length of actuator at its fully extended and retracted positions. The force is max load that a linear actuator can bear and can be rated for both dynamic and static conditions. The rate at which the actuator extends or retracts is known as speed.

For a Stewart Platform to function properly, hydraulic cylinders with servo-valves under position control would offer enough positional accuracy. Additionally, a single piston with a 0.5-inch cylinder may apply a force of up to 589 lb at a standard hydraulic pressure of 3000 psi. Even though they provide the demand for force and positional control, hydraulic systems require a specialised infrastructure and are rather expensive because they involve pumps, filters, valves, hoses, and tubing. Therefore, the Stewart Platform should not use hydraulic actuation.

Pneumatic systems typically produce enough force for this Stewart Platform and may be developed for less money and with less infrastructure than hydraulic systems. However, due to air's compressibility and nonlinear behaviour, pneumatic cylinder positional control is difficult.

After being fine-tuned, even commercially available pneumatic positioning controllers [24] can achieve positional accuracy of just 1 mm (or 0.039 inches). The Stewart Platform is not a good choice for pneumatic actuation because products that match these specifications are more expensive than the project's allocated budget.

Another popular method of linear actuation is ELA. An overview of electric linear actuators(ELA) is provided by Firgelli Automations [10]. They do this by using a gear train to transform a motor's rotational motion into linear motion, which they then link to a nut and lead screw as seen in figure below

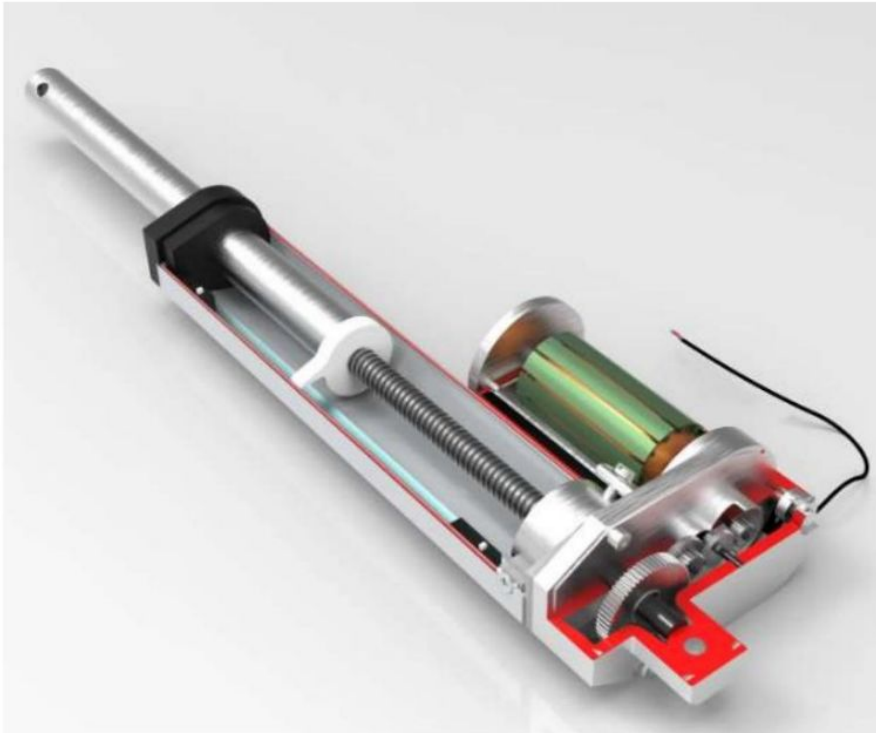


**Fig.7 Section View of an ELA**

When an electric linear actuator reaches its maximum or minimum travel distance, limit switches that are typically factory-installed in the device shut the power to the motor. Linear actuators are

typically driven by 12 VDC motors, while other DC motor voltages and AC motors are also available. A potentiometer is typically used to provide position feedback for some electric linear actuators. The electric linear actuator is ideal for position control since it is less expensive, relatively simple to incorporate, and it can exert mild forces. Electric actuators are the ideal option for this Stewart Platform due to these factors.

There are a number of specifications accessible when selecting electric linear actuators, as was previously mentioned. These requirements were influenced by the project's scope. It's vital to remember that the linear actuator's overall length will be at least twice its stroke when completely stretched. The Stewart Platform will not be used to handle large loads or precisely position machinery; rather, it will be used for kinematics and motion experiments. Actuators with fast speed and low load are therefore the most appropriate for this design

The electric linear actuator PA-14P-8-35 has an 8-inch stroke and a 35 lb dynamic force. The actuator travels at 2 in/sec while drawing 1.0 A when there is no load. The actuator draws its maximum 5.0 A and travels at 1.38 inches per second when fully loaded. It has a potentiometer that gives the Stewart Platform the positional feedback it needs to be controlled. Progressive Automations offers example Arduino code for managing a variety of actuators, including time, current, and more.

## **4.2 Magnetic Spherical Joints**

Depending on how it is set up, the SP contains 6, 9, or 12 passive spherical joints. It was discussed how spherical joints affected the platform's degrees of freedom. A ball joint, like the one in the figure below, is a typical piece of hardware for a spherical joint. A ball joint's swivel angle, which describes the degree of rotation that is possible from the axis of rod to the axis normal, is a feature. This is a crucial feature because the platform operation's range is affected by the ball swivel's range of motion. Most ball joint rod ends have a maximum ball swivel between  $20^{\circ}$  and  $30^{\circ}$ [14], according to the McMaster Carr website.

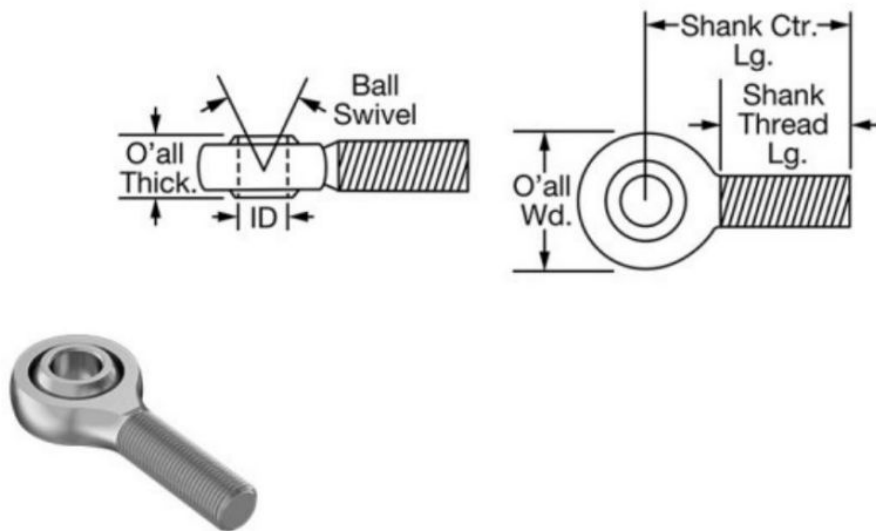


**Fig.8 Ball Joint Rod Ends**

A magnetic spherical joint is an additional option that satisfies the Stewart Platform's spherical joint criterion. As illustrated in the figure below, these spherical joints are made up of a steel ball with a projecting threaded rod attached to it, together with a Neodymium Iron Boron (NdFeB) permanent magnet contained in a cylindrical base. There are several sizes and holding force ratings for the magnetic joints.

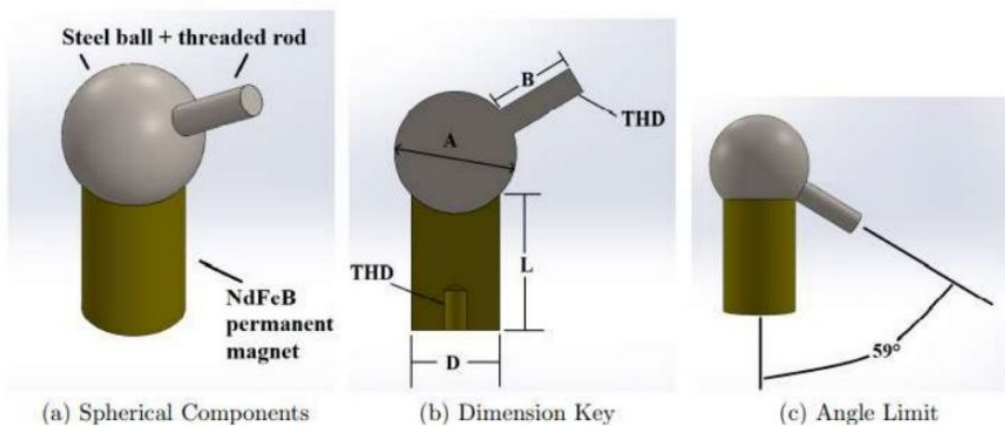




### **Fig.9 Magnetic Spherical Joint Properties**

When choosing the magnetic spherical joint, cost, joints, size and holding force should be taken into account. Typically, all three of these traits rise at the same time. Since 12 joints are required, a less expensive spherical joint is preferred. The requirement for enough holding force needs to be balanced against this. The magnetic joint could separate during normal operation if the holding force is too low, which must be prevented. Additionally, the holding force must not be excessively strong in order for the joint to fail and separate in the event of a binding circumstance. This relieves the acrylic plate loadings while preventing the linear actuator(la) from stopping and overheating. The maximum force the linear actuators are capable of producing is 35 lb, or 156 N.

Although the KD625 appears to fit this requirement precisely, there is not much room for error b/w the actuator force and holding force. The KD310, on the other hand, is the least expensive joint but is outclassed by the la and can only support a small portion of their weight. The KD418 was chosen as the Stewart Platform's holding force solution because it was a reasonable compromise between price, size, and holding force. Using the magnetic joints with this SP has extra benefits. As seen in Figure above, the magnetic ball joints have a ball swivel angle of  $242^\circ$ , which is roughly an order of magnitude bigger than the ball joints discussed earlier. This angle eliminates the joints as a range-limiting issue because it is much greater than the angles of the la relative to the base. Because there was no lubrication between the magnet and steel surfaces at first, friction was a worry. When the steel ball was manually turned against the magnet, friction was highly noticeable and smooth rotation was challenging to achieve. Once the linear actuator was fastened to the joint, the rotation was considerably smoother. This is because pulling the threaded rod or twisting the sphere only results in about an inch of leverage, but the linear actuator offers many inches of leverage. Friction was quite evident and difficult to generate when the steel ball was manually rotated against the magnet. The rotation was noticeably smoother when the linear actuator was attached to the joint. This is such that, in contrast to the linear actuator, which provides many inches of leverage, tugging the threaded rod or twisting the sphere only results in approximately an inch of leverage. When installed on the SP, the actuators effortlessly overcome resistance and revolve smoothly.

### 4.3 Platform

The top and bottom platform plates' top and base platform plates were made of a material that was chosen for its lightweight, low cost, ease of production, and appealing looks. The best material options were aluminium, acrylic, and wood. Lighter plates make the Stewart Platform as a whole lighter even if weight is not essential for this application. The top plate's weight further reduces the platform's capacity to sustain a payload. Despite having lower densities than wood and acrylic, none of the materials offers a measurable weight advantage. Aluminum is stiffer than those two materials, allowing for weight reduction and plate thickness. Wood costs around 2.5x less than acrylic and many times less than Al for the same volume of raw materials. As with Al, Even when the plate thickness is decreased, the relative cost is still much higher. Acrylic is a viable option because of its reasonable weight, low cost, and ease of laser cutting, making it the greatest fit overall.

### 4.4 Shaft Couplers

The coordinated actuation of all six linear actuators in a SP is required. The robot's location and orientation will be inaccurate if they don't. At worst, a significant variation in one or more actuators might force the robot to move out of its boundaries or to take on an unstable attitude, leading to the separation of the magnetic joints. It is clear that actuator accuracy has a significant impact on the SP and parallel robotics. This calls for a mechanical fix known as compliance. A compliant part will permit deviations from its equilibrium when a force occurs on it, but a stiff member will not, as long as the device limits are observed, according to Bram Vanderborght's useful introduction to compliance. [23]

The Plexiglas, linear actuators, and magnetic joints are regarded as stiff components. The acrylic, however, is the least rigid of the three materials, so if the robot finds a binding position or an unexpected loading scenario, the plates will take the strain, increasing the likelihood of deformation and breaking. By connecting a compliant part in series with the la, this can be prevented. The conforming member needs to be packaged neatly and professionally, and it needs to be removable if the SP can function without it.

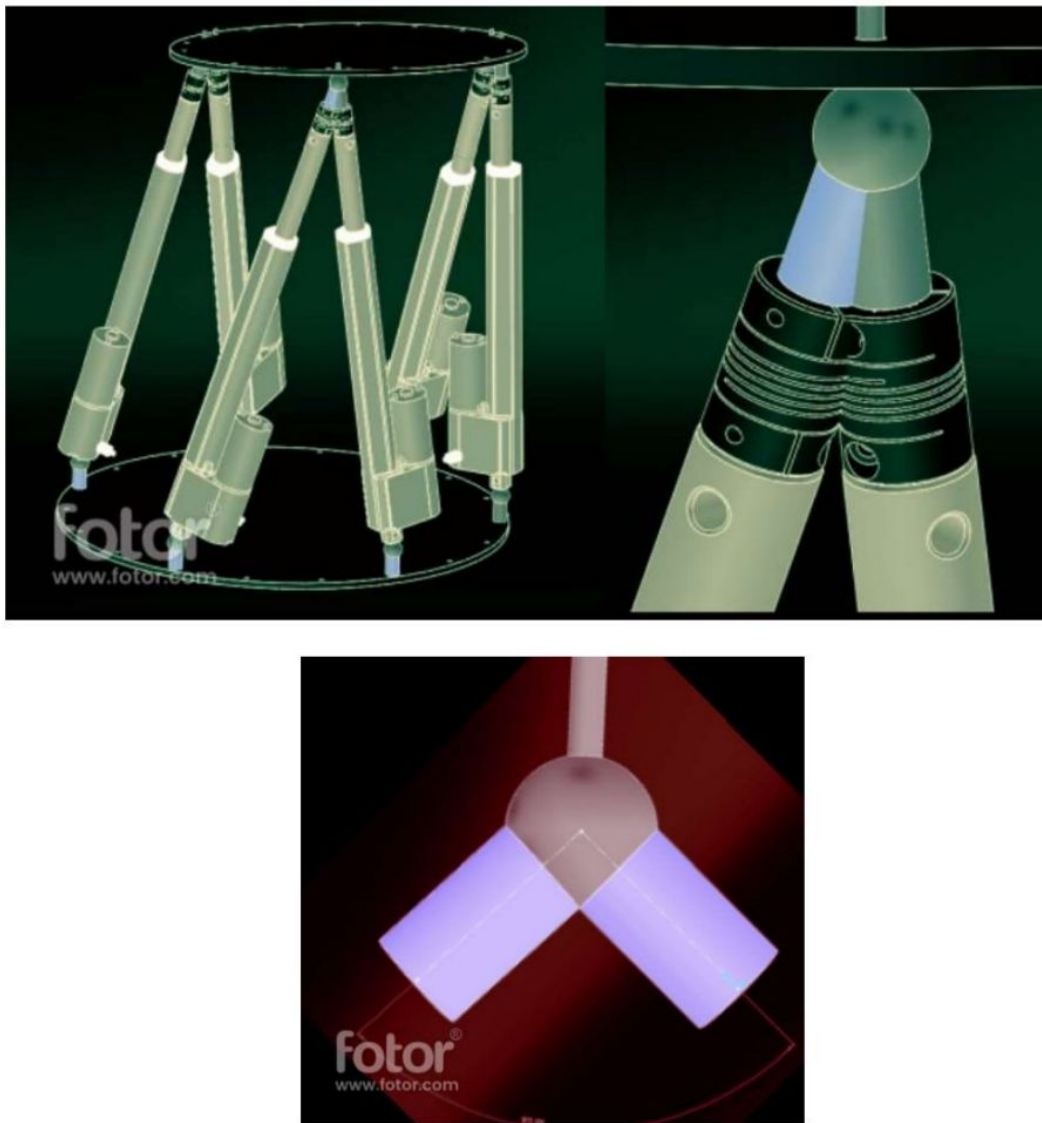
The Compliant part was decided upon by using helical shaft couplings because they met the aforementioned criteria. They are primarily designed for torque transmission, as seen in the figure below, although they are flexible enough to give the required compliance in axial and bending motions. One option for shaft couplings is a WAC20-4mm-4mm Aluminum Alloy Couplings.



Fig.10 Helical WAC20mm-4mm-4mm Couplings

#### **4.5 Stewart Platform ( 6-3 Configuration )Geometry**

The three top joints are evenly spaced at  $120^\circ$  angles, while the six base joints are uniformly spaced at  $60^\circ$  degrees in a 6-3 configuration. In this setup, two actuators must share a joint. This can be done by attaching two magnets to a single steel ball, as seen in the interference pattern in Figure below, where the Stewart Platform is positioned and oriented normally. Only when two magnetic joints' cylindrical axes are more than  $92.9^\circ$  apart, as indicated in Figure below, can a spherical joint be shared by both of them. It is feasible outside of the SP's range of motion only. Therefore, the steel ball cannot be shared by the joints' magnetic components.



**Fig.11 Motion Limitation Range with Sharing Spherical Joint**

The s-joints have to be divided in order to correct this. With separation, the robot will only be roughly in a 6-3 configuration. Figure following illustrates how the spheres' shape determined the 3.47° angle separation from the 120° centerline between each joint. The joint angles for the

6-3 configuration are no longer at  $120^\circ$  as a result of this solution's angle of separation. The Stewart Platform's modelling and kinematic equations must take this joint angle into account.

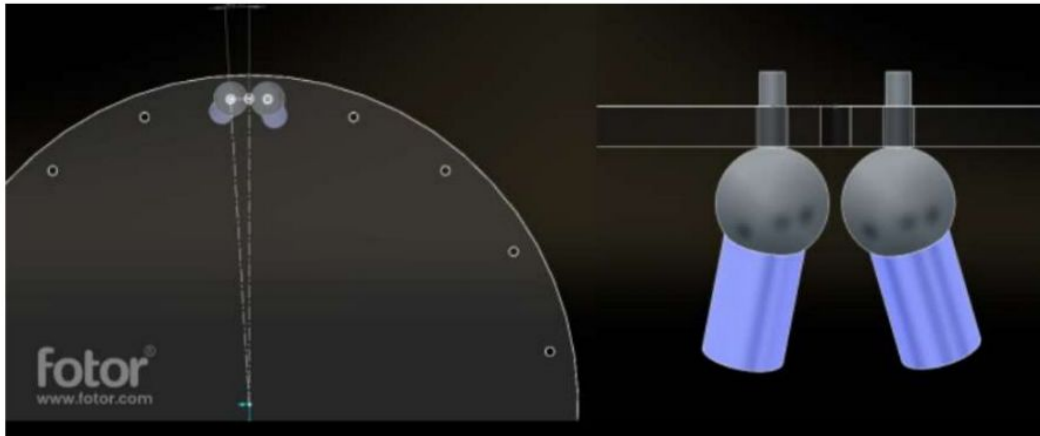


**Fig.12 Joint Angle of Spherical Joint in 6-3 Configuration**

#### 4.6 Electronics Enclosure

The Stewart Platform needs a few essential electronic parts in order to function. A power source, microprocessor, motor driver, as well as connecting ports, plugs, and switches, are among these parts. For security and dependability, the components must be encased in an electronics enclosure, shielding users from contact with the live power and internal components from negligent or unintentional handling. The enclosure should ideally provide adequate airflow, be reasonably light and portable, and be simple to make at a cheap material cost. Additionally, using the provided 6-pin connector to connect potentiometer and PA-14P motor to the enclosure is a suitable option. The choice of sheet metal for the electronics enclosure was made due to its low cost, high strength, and ease of manufacture. 3D-printed plastic enclosures or acrylic were alternatives that were taken into consideration. The enclosure will be fastened to the Stewart Platform's base underneath, completing the assembly of SP and its electronics.

The electronics enclosure's bottom holds the power supply. The Arduino due and motor driver are suspended above it, which keeps the enclosure small. The wall thickness of the enclosure walls where the 6-pin Molex connectors were put may not be enough to hold the connections in



place. The connector would be forced back into the enclosure when the linear actuator was connected in, making it hard to move it back into position once it was mounted beneath the Stewart Platform base. When the connectors are inserted into the linear actuators, the connectors will stay in place thanks to retainers that can be printed to thicken the wall. These retainers also provide a permanent labelling option that makes it impossible to change or delete the actuator number.

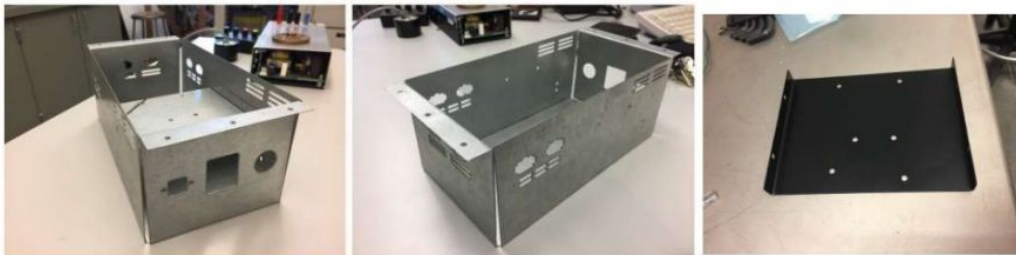


**Fig.13 Examples of Electronic Enclosure and Arduino due Mount**

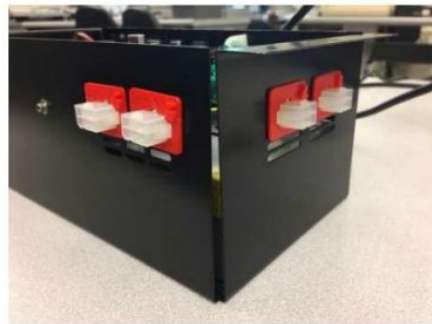


**Fig.14 Molex Connector Retainer and Label**

## **Chapter 5**

### **Electronic Design**

The Stewart Platform's electronic layout must accommodate the robot's operational requirements. Power is required by the robot to move the actuators, and these movements must be precisely

planned and regulated. Based on computed inputs and the present locations of the linear actuators, a controller can implement a control loop and deliver actuation signals.

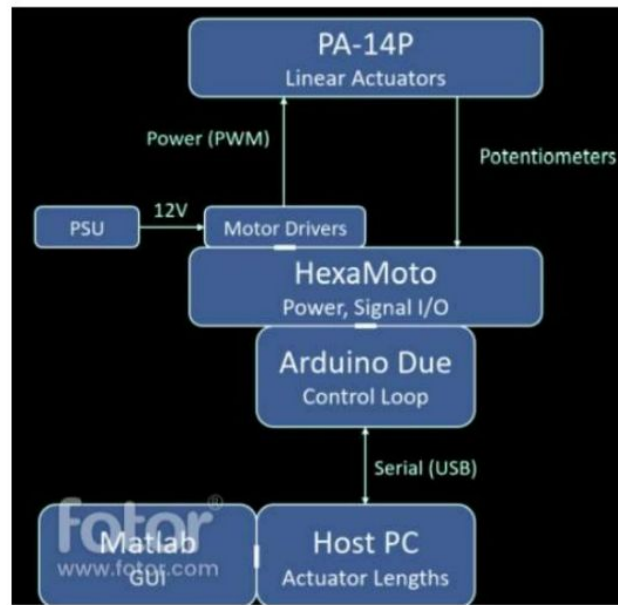


**Fig .15 Stewart Platform System Design**

Above figure provides a high-level system overview. The PA-14P actuators are located at the top of the diagram. The designs and implementation of the middle section, electronics, are covered in this chapter. The main electronic parts are a controller, motor drivers, and a power supply. The user interface for the Stewart Platform and the controller's source code are both included in the diagram's bottom section.

## 5.a Microcontroller

A microcontroller creates a computer on a chip using a microprocessor , RAM, ROM, and i/o capabilities . They are often utilised as a functional component of an electrical or mechanical system. This is an example of an embedded system, which is frequently constrained by real-time requirements. The Stewart Platform can be controlled by any number of microcontrollers.



### 5.a.1 Microcontroller Selection

For a number of reasons, an Arduino board was selected as the microcontroller platform to control the robot. Typically, Arduinos are used in a user-friendly prototyping environment made up of makers, hobbyists, students, and others. An Arduino platform is a good fit for the Stewart robot because to its configuration, intended use, and target market. The software and design of the board are open-source, giving room for any necessary adjustments. In order to add new features or adjust performance for a particular application, current board designs and hardware might be modified. Although the StewartPlatform did not require any hardware adjustments, having this option was advantageous in case it did later in the design process. The ease of replacing while utilising an Arduino is an additional advantage. If the Arduino board breaks, you can order a replacement within a few days. installing a pre-made board, then downloading the project to the new board. This approach to changing the microcontroller is practically hassle-free.

A variety of boards from Arduino are available, each with varied features and performance. The Nano, UNO, Due, and Mega are a few boards. The chosen board must have a min no. of required i/o accessible. Since the PA14P actuators have potentiometers on each one, there must be six analogue inputs in order to read the actuators' positions. The PWM pin and the direction pin are used by the motor driver to output electricity at a specific level and polarity. An Enable and Disable pin is likewise shared by the motor drivers. This required 14 digital outputs, all of which had to be PWM-capable. Both requirements are met by the Due and Mega 2560 Arduino boards. Regarding I/O capabilities, they are quite comparable, but their features differ. At the same price, the Due provides a clock that is 5.25 times faster than the Mega 2560, 2 times as much flash memory, 12 times as much SRAM. Fig below depicts the Due, the microcontroller chosen to operate the Stewart Platform.



(a) Isometric View



(b) Top View

**Fig.16 Arduino Due**

### 5.a.2 Arduino Due Specifications

Feature	Value
Microcontroller	AT91SAM3X8E
Operating Voltage	3.3V
Digital I/O Pins	54
Analog Input Pins	12
Analog Output Pins	2
Flash Memory	512
SRAM	96 KB
Clock Speed	84 MHz

**Table 1.Arduino Due technical Specifications**

One characteristic that sets the Arduino Due apart is its two USB connections. The Due's web page on the Arduino website states that one port is a Programming port and the other is a Native port. In addition to providing a virtual UART.COM port to a connected computer, an ATmega16U2 connected to the programming port creates a hardware UART connection with the SAM3X. When the Native USB is connected to the SAM3X, serial communication over USB is enabled. The Native port can also act as a USB host or emulate other USB devices. Both ports can be used to programme the Due, although there are several key distinctions. When the Programming port is opened and connected at 1200 baud, a SAM3X "hard-erase" procedure is

performed. Activating the Erase and Reset pins before UART transmission, whether open or closed.

In contrast, a "soft-erase" process is carried out when the Native port is opened and closed at 1200 baud. After cleaning the flash memory, the bootloader resets the board. It is advised against using the soft-erase method after the microcontroller has crashed in favour of programming through the Programming port. The 115200 baud rate restriction on the Programming port, however, can be an issue if high-speed serial connection is required. The Arduino sketch's baud rate setting is disregarded because the Native port can handle far faster serial communication rates thanks to the USB connection. Programming and use of the robot were very different in terms of functionality and output. The Native port was significantly faster at uploading code than the Programming port. However, due to its dependability, the Programming port was used when uploaded sketches crashed. The Native port was utilised for typical operations, functioning, and data transmission [3].

## **5.b HexaMoto Shield**

A second motor driver board is required to complete the electronic hardware design since the Arduino Due can control motors through its PWM outputs but does not have the hardware to power them. You have two choices: buy an aftermarket motor driver board, or create and put together a bespoke board.

### **5.b.1 Design Requirements**

Each linear actuator will require six channels on the motor driver shield. Every motor driver is required to employ a speed limiter. If the actuators could only work at their peak speed, the robot operation would not be acceptable. It would also be helpful to obtain the potentiometer signals from the Arduino shield. In this case, all inputs and outputs, save the 12V motor supply, would connect with the Arduino Due via the shield, offering a whole solution.

The analogue output of a potentiometer is a voltage. Eight bit digital-to-analog converters (ADCs) may output 256 different values. The potentiometer's ADC measurement translates each minute fluctuation into a length of 0.0156 inches for a 4-inch stroke. The measurement is 0.0469 inches for a 12-inch stroke. A 10-bit ADC that generates 1024 values

similarly shows that each increment translates to a change in length of 0.004 inches for a stroke that is 4 inches long and 0.012 inches for a stroke that is 12 inches long. ADCs are not totally accurate to the aforementioned values since they have causes of measurement error.

The DC linear actuator from Progressive Automation will have a potentiometer and five wires for integrating electronics.

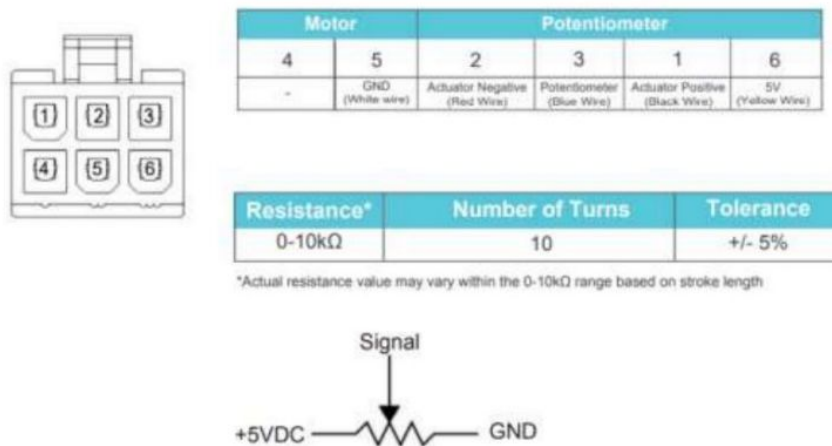


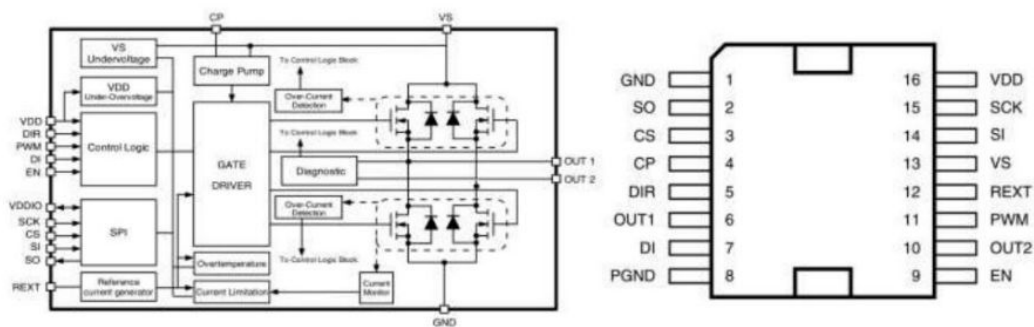
**Fig.17 Progressive Automation PA-14P Pinout [19]**

### 5.b.2 HexaMoto Design

The HexaMoto's design complies with all of the requirements listed above. It uses six L9958SBTR motor drivers, 13 screw terminals for I/O, and pin headers to connect to the Arduino Due.

JLCPCB provided two-layer boards that were less than 100mm x 100mm for \$2 for quantity five after researching a number of PCB providers. The HexaMoto's overall size was determined by this. They will be positioned around the centre plane because the shield must by necessity have pin headers that match the Arduino due. The perimeter of the bottom half of the board will be surrounded by motor drivers and their screw terminals, and the perimeter of the top half of the board will be surrounded by potentiometer screw terminals.

The board needs to be capable of handling up to 5A per motor channel in order to eliminate resistance. Polygons may be used to transfer this high current rather than standard traces. The screw terminal in the middle of the board distributes the 12V input from the power source to the motor drivers through the 50-100+ mil wide polygons.



The inputs EN, DI, PWM, and DIR are used to control the aforementioned motor driver. Whether the bridge is set to Tri-state or On-state is determined by the EN (enable) and DI (disable) pins. The associated motor's direction and speed are managed by the DIR (Direction) and PWM (Pulse Width Modulation) pins. This motor driver did not make use of or have a connection to the serial peripheral interface (SPI).

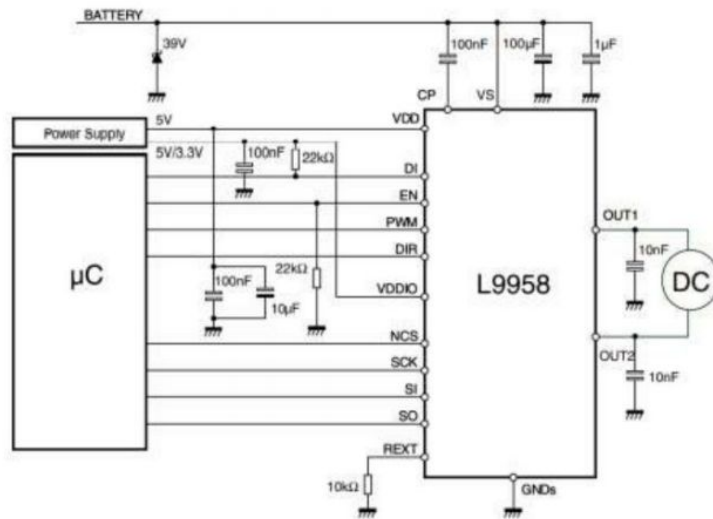


**Fig.19 L9958 Application Circuit [22]**

On the HexaMoto Shield, all relevant resistors and capacitors will be present. Decoupling capacitors in the amount of 10 nF are placed on the outputs to lessen high frequency noise. To increase the robustness of the output short protection, the 100F and 1F capacitors connected to Vs are used for decoupling.

### 5.2.3.b I/O Hardware Components

The cable of the linear actuator was attached using screw terminals. The six outputs from the linear actuator motors and the input voltage from the DC power supply unit will both be linked to two-position screw terminals. The potentiometer for the linear actuators is attached using three-position screw connections as shown below. It is made up of the sensor, GND, and 3.3 volts. The HMS and ArduinoDue are connected using straightforward pin headers. In the image



below, typical 0.10 inch pin headers are seen. Because the Arduino Due runs on +3.3VDC logic rather than +5VDC, a separate voltage is used for the potentiometer..

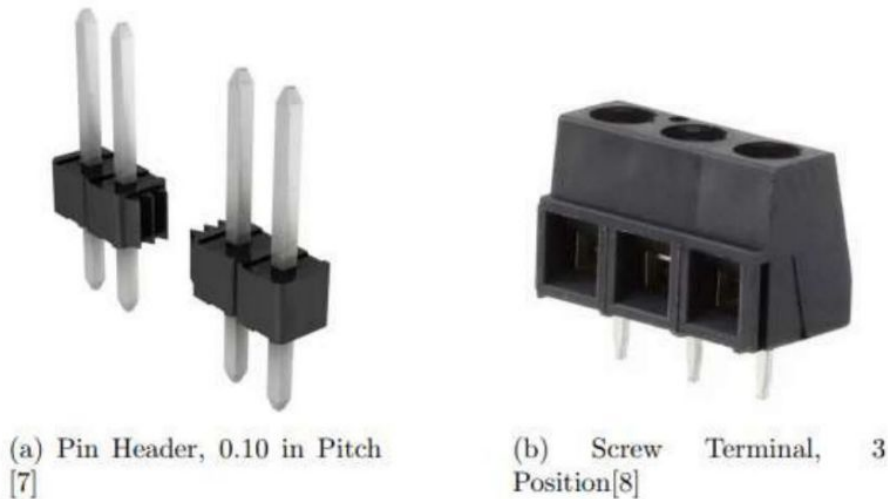


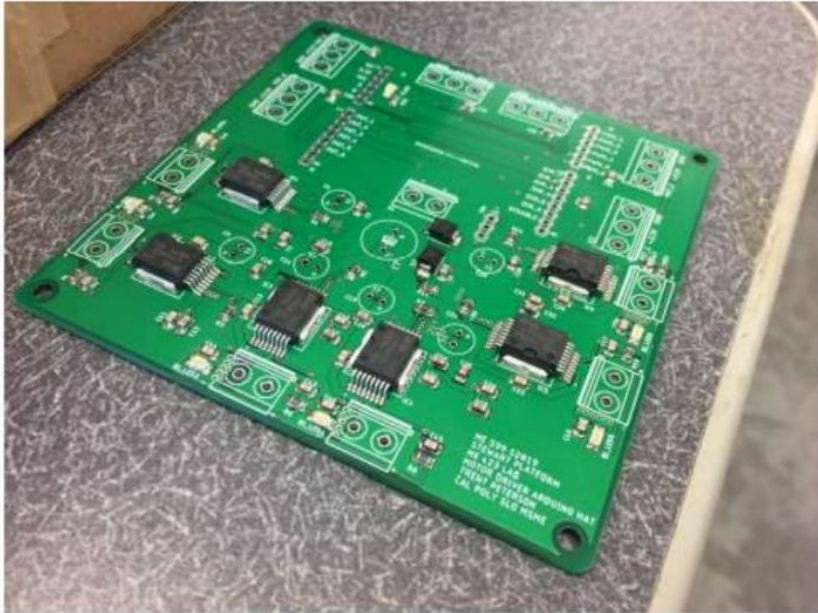
**Fig.20 HMS I/O Hardware**

### 5.c HMS Assembly

Soldering was necessary for the HMS assembly of through-hole and surfacemount components. Because they are bigger, more manageable, and allow for soldering on the other side of the circuit board, through-hole components are typically simpler to solder. Smaller package sizes may make surface mount components more challenging to utilise. In this application, solder paste, a stainless steel stencil, and an oven were also used to connect surface-mount components. Metal sheet that has been laser cut to mimic the solder pads on the PCB is used as the stencil. A little, uniform quantity of solder paste is applied to each pad when it is applied to the stencil and spread out. As the solder paste is placed to the stencil and dispersed, a small and consistent amount of solder paste is deposited on each pad. The PCB is heated in an oven after the components are attached to it so that the solder can reflow. After cooling and reflowing, the HexaMoto Shield is shown in the illustration below. The skin, eyes, and respiratory system may become irritated by solder paste, it should be mentioned. Handle solder paste carefully to prevent getting it in your eyes, on your skin, or inhaling the fumes. When using isopropyl alcohol, used



to clean up solder paste.. Fig.21



### : HexaMoto Shield, Post Solder Paste Application and Reflow

After applying a tiny amount of uniformly dispersed solder paste to each pAfter that, the HMS was manually connected to the pin headers, capacitors, screw terminals. These through-hole pieces are not meant to be used with the stencil. The HexaMoto Shield was totally built after soldering, as seen in the image below. Before proceeding to the next level of integration, all traces were examined for continuity and brevity. The HexaMoto Shield was constructed and verified for compatibility with the Arduino Due. Although theoretically possible, using the TX pin as a general-purpose digital I/O pin in real-world applications is not practicable. The transmit pin is labelled as TX for serial communication. As a result, the TX pin's trace was broken, and a jumper wire was used to connect it to a free pin header.

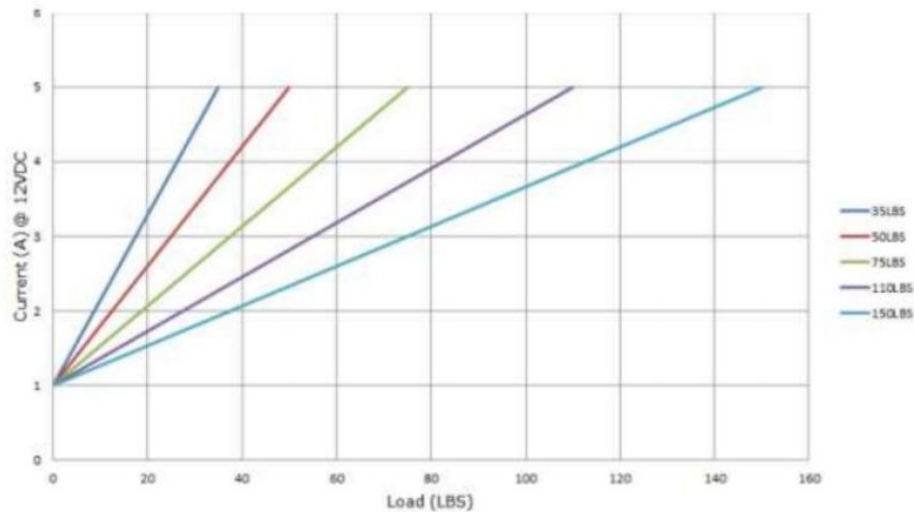
**Fig 22.Hexamoto shield completed**



#### **5.d DC- Power Supply(PS)**

Each la needs to be powered enough in order to work effectively. According to PA(Progressive Automations), each la consumes a min of 1A when there is no load and up to 5A when there is a

maximum load, as seen in the figure below.



a ps unit chosen to accommodate the system's max current draw. 30A would be drawn if all linear actuators simultaneously encountered their max load. The PSU also includes an integrated fan that always runs when it is powered.

As a result, hot air is expelled via the front of the unit and supplied at the unit's back. Extended cycle periods did not result in elevated temperatures.

## 5.e Connectors

Through a fused power entry receptacle, the PS unit will be connected to AC power. The receptacle is depicted in Figure below . Before the power supply, the live AC wire will be linked in series through a switch, enabling the Stewart Platform power to be toggled without unplugging. The power outlet also features a fuse, which increases user safety and guards against harm to the robot in the event of a short. A USB-B cable that fits into the electronics enclosure's

USBB port links the PC host to the Arduino.



(a) Power Receptacle



(b) USB-B Receptacle

Micro-USB is required for the Arduino Due. As seen in Figure below, a micro-USB cable was attached to the USB-B receptacle. The host PC and the AD(Arduino Due) are connected through this as an intermediary device.



## **Chapter 6**

### **Conclusion and future work**

One of the best methods for treating lung cancer is radiation therapy. The tumour and surrounding tissue are exposed to radiation during traditional radiation therapy. This mechanism causes damage to healthy cells. In order to better understand the size and position of the tumour, radiation therapy has evolved to image guided radiation therapy, in which images from various imaging tests are studied both before and after the treatment.

In this project ,we got to know about the stewart platform and its applications.A stewart platform with 6-3 configuration has been proposed and discussed the mechanical design and Electric design up to some point.Further it need a software design on Image Processing of CT scan of lung and 3d print of the equipments required.Thus the stewart platform can be used to mimic the movement of tumor .



## References

<https://www.tandfonline.com/doi/abs/10.1586/14737140.7.1.89>

[https://www.radiologyinfo.org/en/info/intro\\_onco](https://www.radiologyinfo.org/en/info/intro_onco)

[3] Arduino. ARDUINO DUE, 2019. Accessed 22 June 2019.

[4] K. J. Ayala. The 8051 microcontroller. Cengage Learning, 2004.

[5] P. Cruz, R. Ferreira, and J. Silva Sequeira. Kinematic modeling of stewart-gough platforms. ICINCO, 2005. [

6] B. Dasgupta and T. Mruthyunjaya. The stewart platform manipulator: a review. Mechanism and Machine Theory, 35(1):15–40, December 1998.

[7] Digi-Key. Molex 0022284060. Web, August 2019. Accessed 18 August 2019.

[8] Digi-Key. Molex 0398800303. Web, August 2019. Accessed 18 August 2019.

[9] Digi-Key. SunLED XZMDKVG55W-4. Web, August 2019. Accessed 18 August 2019.

[10] Firgelli Automations Team. Linear Actuators 101 - Everything you need to know about Linear Actuators. Web, November 2018. Accessed 13 June 2019.

[11] IBS Magnet. Magnetic ball joints, 2019. Accessed 13 June 2019

. [12] K. Lancaster. AMiBA Radio Telescope. Web, June 2006. Accessed 10 January 2020. 69

[13] Matthewbarry. Eric gough's tire testing machine. Web, March 2016. Accessed 10 January 2020.

[14] McMaster-Carr. Ball Joint Rod Ends Datasheet, 2019. Accessed 13 June 2019.

[15] J. Merlet. Parallel Robots. Springer Netherlands, P.O. Box 17, 3300 AA Dordrecht, The Netherlands, 2006.

[16] S. B. Niku. Introduction to Robotics: Analysis, Control, Applications. John Wiley and Sons, 2nd edition, 2011.

[17] S. B. Niku. Introduction to Robotics: Analysis, Control, Applications. John Wiley and Sons, 3rd edition, 2020.

- [18] Progressive Automations. Multimoto arduino shield. Web, August 2019. Accessed 18 August 2019.
- [19] Progressive Automations. PA-14P Datasheet, 2019. Accessed 13 June 2019.
- [20] Progressive Automations. Resources. Web, August 2019. Accessed 19 August 2019.
- [21] Robot Power. Multimoto product information. Web, August 2019. Accessed 18 August 2019
- [22] STMicroelectronics. L9958, December 2013. Accessed 20 August 2019.
- [23] B. Vanderborght. Compliant robots. Web, January 2012. Accessed 10 October 2019.
- [24] S. Vincent and J. Bridges. Positioning with air electropneumatic-positioning systems bring extreme accuracy to high-speed automation. Web, April 2015. Accessed 13 June 2019.



# Varkala\_BTP

## ORIGINALITY REPORT

18%

SIMILARITY INDEX

18%

INTERNET SOURCES

1%

PUBLICATIONS

%

STUDENT PAPERS

## PRIMARY SOURCES

1

[digitalcommons.calpoly.edu](https://digitalcommons.calpoly.edu)

Internet Source

16%

2

[core.ac.uk](https://core.ac.uk)

Internet Source

1%

3

[www.oncolex.org](https://www.oncolex.org)

Internet Source

<1%

4

[ascopubs.org](https://ascopubs.org)

Internet Source

<1%

5

[www.bannerhealth.com](https://www.bannerhealth.com)

Internet Source

<1%

6

[www.mskcc.org](https://www.mskcc.org)

Internet Source

<1%

7

Chenyu Liu, Hailiang Chen, Hengjun Zhou, Simiao Yu, Ning Wang, Weihe Yao, An-Hui Lu, Weihong Qiao. "Magnetic Resonance Imaging-Guided Multi-Stimulus-Responsive Drug Delivery Strategy for Personalized and Precise Cancer Treatment", ACS Applied Materials & Interfaces, 2021

Publication

<1%

8	du Plessis, L.J.. "An optimally re-configurable planar Gough-Stewart machining platform", Mechanism and Machine Theory, 200603 Publication	<1 %
9	www.ncbi.nlm.nih.gov Internet Source	<1 %
10	New Trends in Mechanism Science, 2010. Publication	<1 %
11	backend.orbit.dtu.dk Internet Source	<1 %
12	images-se-ed.com Internet Source	<1 %
13	Liuyun Gong, Yujie Zhang, Chengcheng Liu, Mingzhen Zhang, Suxia Han. "Application of Radiosensitizers in Cancer Radiotherapy", International Journal of Nanomedicine, 2021 Publication	<1 %

Exclude quotes On

Exclude matches < 5 words

Exclude bibliography On